

Angiogenesis in Calcium Phosphate Scaffolds by Inorganic Copper Ion Release

Jake Barralet, Ph.D.,¹ Uwe Gbureck, Ph.D.,² Pamela Habibovic, Ph.D.,¹ Elke Vorndran, M.Sc.,²
Catherine Gerard, Ph.D.,³ and Charles J. Doillon, Ph.D., M.D.³

Angiogenesis in a tissue-engineered device may be induced by incorporating growth factors (e.g., vascular endothelial growth factor [VEGF]), genetically modified cells, and/or vascular cells. It represents an important process during the formation and repair of tissue and is essential for nourishment and supply of reparative and immunological cells. Inorganic angiogenic factors, such as copper ions, are therefore of interest in the fields of regenerative medicine and tissue engineering due to their low cost, higher stability, and potentially greater safety compared with recombinant proteins or genetic engineering approaches. The purpose of this study was to compare tissue responses to 3D printed macroporous bioceramic scaffolds implanted in mice that had been loaded with either VEGF or copper sulfate. These factors were spatially localized at the end of a single macropore some 7 mm from the surface of the scaffold. Controls without angiogenic factors exhibited only poor tissue growth within the blocks; in contrast, low doses of copper sulfate led to the formation of microvessels oriented along the macropore axis. Further, wound tissue ingrowth was particularly sensitive to the quantity of copper sulfate and was enhanced at specific concentrations or in combination with VEGF. The potential to accelerate and guide angiogenesis and wound healing by copper ion release without the expense of inductive protein(s) is highly attractive in the area of tissue-engineered bone and offers significant future potential in the field of regenerative biomaterials.

Introduction

ANGIOGENESIS IS A MAJOR, but transitory, event during the formation of wound tissue. Similar events also occur on the surface and/or the interior of a scaffold used to repair or replace a tissue defect. Prompt blood supply into a tissue-engineered device can improve the survival of preseeded cells and subsequent tissue integration, and enhance the success rate of the implant/graft similar to that achieved using an autograft.¹⁻⁴ Angiogenesis is essential for osteoblast cell survival and osteogenesis as well as for the regulation of bone remodeling and fracture repair in the long term.^{5,6} Bone wound healing may be stimulated by releasing growth factors such as bone morphogenetic proteins into the bone defect.⁷ Similarly, blood vessel development can be triggered by angiogenic growth factors such as vascular endothelial growth factor (VEGF) or fibroblast growth factor-2 (FGF-2) released from an implant to induce and accelerate vascularized tissue growth⁸ as recently demonstrated in a bone defect.⁹ Because a high concentration of growth factor(s) may

be required (usually in the order of μg) and growth factor bioactivity may only last for a short period due to their inherent instability, their full regenerative potential may not always be reached. In response to these shortcomings different strategies have been proposed to provide sustained release such as using biodegradable fibrin or collagen scaffolds, by mixing with polymers (e.g., polyglycolic and polylactic acid) before processing, or by a preencapsulation of growth factors in microspheres that were then incorporated into a scaffold.^{10,11} However, the use of high doses of recombinant protein is not ideal in terms of cost, preservation until use, and safety.

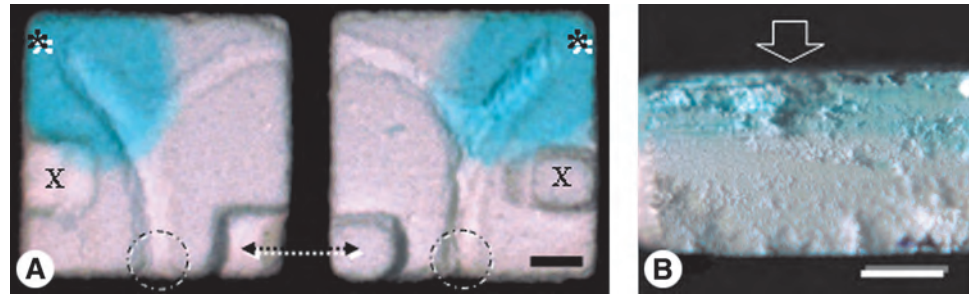
Copper has been shown to enhance proliferation of endothelial cells and angiogenesis *in vivo*,¹²⁻¹⁴ and is known to modulate angiogenesis as demonstrated by its dietary elimination being a potential antiangiogenic strategy in cancer treatment.¹⁵ The copper content of wound tissue participates in the mediation of the generation of free radicals in regenerating tissues,¹⁶ and it is also essential for bone metabolism and turnover in normal growth and development of

¹Faculty of Dentistry, McGill University, Montreal, Quebec, Canada.

²Abteilung für Funktionswerkstoffe der Medizin und der Zahnheilkunde, ZMK-Klinik, Universität Würzburg, Würzburg, Germany.

³Department of Surgery, Université Laval, and Oncology and Molecular Endocrinology Research Centre, CHUL Research Centre, Quebec City, Quebec, Canada.

FIG. 1. Design of the porous DCPD scaffold with a large and small open pore (dashed circles and unmarked, respectively) and a closed pore (asterisk). A 1 mol/L copper sulfate solution (5 μ L) was deposited on the closed branch (asterisks) of a printed Y-shaped pore on each 8-mm² DCPD half material to visualize the diffusion of the solution through the microporous scaffold (A; scale bar = 2 mm). Note that respective halves press-fit together, aligned by two cubic anchors (X and double-head arrow). The materials were then sectioned transversally through the center of the closed branch (arrow) (B, scale bar = 1 mm). Color images available online at www.liebertonline.com/ten.



the skeleton.¹⁷ Previously, copper has been complexed to a crosslinked hyaluronic acid-based hydrogel that significantly enhanced endothelial cell migration and chemoattraction *in vitro*, compared with copper chloride alone.¹⁸ This composite hydrogel was encapsulated by fibrotic tissue upon subcutaneous implantation in which vascularity was increased in the presence of copper.¹⁹ Recently, there have been several reports demonstrating that VEGF-loaded scaffolds are able to accelerate bone repair in irradiated healing-compromised models and in critical-sized defects.^{20–22}

The aim of this study was to further examine the angiogenic potential of copper ions, this time adsorbed onto a degradable osteoconductive macroporous scaffold and directly compare it with VEGF. We present a detailed study of the use of copper ions as angiogenic agents in brushite ceramics and investigate the effect of doses of copper sulfate compared with VEGF and combinations of copper ions and VEGF.

Materials and Methods

Scaffold design and manufacture

A Y-shaped hemicylindrical pore was designed in the x - y plane of dicalcium phosphate dehydrate (DCPD) cuboids with dimensions 8 \times 8 \times 2 mm using a CAD drawing package. Scaffolds were made in two mirror image halves that keyed into one another to form a Y-shaped pore, closed at one of the branched ends (Fig. 1A) that were designed to press fit together to form a block containing the model macropore. Three-dimensional printing was used to form DCPD components as described previously.²³ Briefly, a 3D powder printing system (Z-Corporation, Burlington, MA) with a 55 wt% β /45 wt% α Tricalcium Phosphate (TCP) powder and 20% phosphoric acid binder and an anisotropic scaling $x = y = z = 1.0$ was used to print components using a layer thickness of 0.1 mm. Printed components were stored in 20% H₃PO₄ for three times of 60 s.

Copper sulfate adsorption and copper ion release

Copper sulfate solution was adsorbed onto Y-shaped scaffolds at concentrations ranging from 0.35 to 0.035 mmol/L (Table 1 and Fig. 1). Five microliters of the solution was deposited on the center of the branched end of each half of the scaffold followed by drying at room temperature for 24 h. To measure *in vitro* copper ion release, one half scaffold was immersed in either 10 mL phosphate-buffered saline (PBS) or bovine calf serum at 37°C ($n = 3$ per

concentration). The solutions were refreshed daily and analyzed by ICP-MS (Varian, Darmstadt, Germany) against standard solutions of 0, 50, and 100 ppb copper. Serum was in contact with the scaffold during the whole incubation period without any rinse; copper concentrations were measured in collected serum, and background copper concentration obtained from fresh serum was subtracted to give the amount of copper released (average of $n = 3$).

Scaffold loading

Murine VEGF (R&D, Cedarlane Laboratories, Burlington, Canada) was used at doses of 0.2 and 2 μ g per scaffold distributed in 5 μ L on each mating half over the closed macropore branch. Similarly, 5 μ L of copper sulfate (Sigma-Aldrich Canada, Oakville, Canada) containing 5600, 560, or 56 ng was absorbed on each half of one scaffold. VEGF and copper sulfate solutions were also combined at 0.2 μ g and 56 ng per scaffold, respectively. Control scaffolds were treated with the vehicle solution (Hank's balanced salt solution).

Implantation

All animal experiments were performed according to the guidelines of the Canadian Council for Animal Care and approved by our institutional Animal Care Committee. Materials were sterilized by 70% alcohol bath followed by a rinse in NaCl-HEPES buffer and then by Hank's balanced salt solution before angiogenic factor loading and

TABLE 1. IMPREGNATION OF BRUSHITE SCAFFOLDS WITH CuSO₄ SOLUTION AT DIFFERENT CONCENTRATIONS

CuSO ₄ concentration of impregnation solution	CuSO ₄ deposited per scaffold (μ g)	Cu ²⁺ load per scaffold (ng)
0.35 mol/L (56 mg/mL)	560	222,900
35 mmol/L (5.6 mg/mL)	56	22,290
3.5 mmol/L (0.56 mg/mL)	5.6	2229
0.35 mmol/L (0.056 mg/mL)	0.56	222.9
0.035 mmol/L (0.0056 mg/mL)	0.056	22.29

Every scaffold was impregnated with a total volume of 10 μ L (5 μ L per half). CuSO₄, copper sulfate.

implantation. In sterile conditions, each 8-mm² implant half was secured by a propylene thread around the implant. Under anesthesia, an intraperitoneal implantation was performed by insertion of the implant directly in the peritoneal cavity (one scaffold per animal). The peritoneum and abdominal muscle were sutured separately to the skin closure. All animals were sacrificed by day 15. At least three animals were used for each condition.

Observation

At sacrifice, the scaffold was retrieved and opened to expose the interior of the implant halves that remained tightly sealed throughout implantation, and tissue response was photographed. Removal of tissues from the pore (channel) may have led to bleeding; thereby, the lengths of capillaries were assessed *in situ* immediately after specimen retrieval. Macroscopic examination (5×) of the newly formed tissue invading the Y-shaped pore was used to provide information on the extent of vascularization. Red areas of tissue were screened to determine whether they were clots or vascularized areas, based on the observation of multiple specimens and their corresponding histological sections and immunohistochemistry. Microvessel invasion along the pore structure was directly measured on the magnified macro views by tracing the extension of blood-filled microvessels visible from the main open pore toward the closed end pore for each scaffold half. Blinded measurements were performed in triplicate and separately.

After fixation in zinc fixative (10 mmol/L TRIS buffer, pH 7.4; 3 mmol/L calcium acetate; 22.8 mmol/L zinc acetate; and 36.7 mmol/L zinc chloride), newly formed wound tissues in the macropore branches and in the main pore were excised. Histological sections were processed through paraffin embedding, and stained with hematoxylin–phloxin–safran.

Immunohistochemistry

Unstained zinc-fixed tissue sections were deparaffinized and rehydrated. Tissues were treated with 3% hydrogen peroxide, and then blocked with a blocking reagent containing rat serum in PBS (Chemicon International, Cedarlane, Ontario, Canada). After a brief wash, primary antibody toward murine CD31 (rat anti-mouse CD31 monoclonal antibody; BD Pharmingen, Invitrogen, Ontario, Canada) was applied at a 1/50 dilution. After 3-h incubation at room temperature, tissues were rinsed (3× TRIS-buffered saline [TBS] solution containing 0.1% Tween20) and a secondary antibody (Biotin-conjugated goat anti-rat Ig polyclonal antibody; BD Pharmingen, Invitrogen) was applied at a 1/50 dilution. After incubation, tissues were rinsed again (3×TBS), and a solution of streptavidin–horse radish peroxidase was applied, followed by a final rinse (3×TBS). A fresh solution of 3,3′ diaminobenzidine in TBS was applied to reveal the antibody reactivity. Negative control sections were processed in parallel, except that the primary antibody incubation was replaced by PBS solution. Slides were washed in water and observed under microscopy without counter stain.

Statistical analysis

One-way analysis of variance was used for statistical analyses, and the multiple comparisons among the different

groups were made using the Duncan’s method. A probability value <0.05 was considered to denote statistical significance.

Results

Copper sulfate–impregnation and copper ion release from DCPD scaffolds

To visualize the impregnation of a 5 μL copper sulfate solution into the microporous cement, a high dose that was visibly blue was loaded at the closed end of the macropore on the surface of DCPD materials. Adsorption and penetration of copper sulfate appeared diffuse and uniform around the pore (Fig. 1A) as well as in the interior of the materials after sectioning (Fig. 1B).

Copper release profiles for different concentrations of copper sulfate in PBS and serum are illustrated in Figure 2. In PBS, although the concentration of the impregnation liquid and therefore the total amount of deposited copper varied over a range of four orders of magnitude, the released amounts were found to be only marginally different (Fig. 2A).

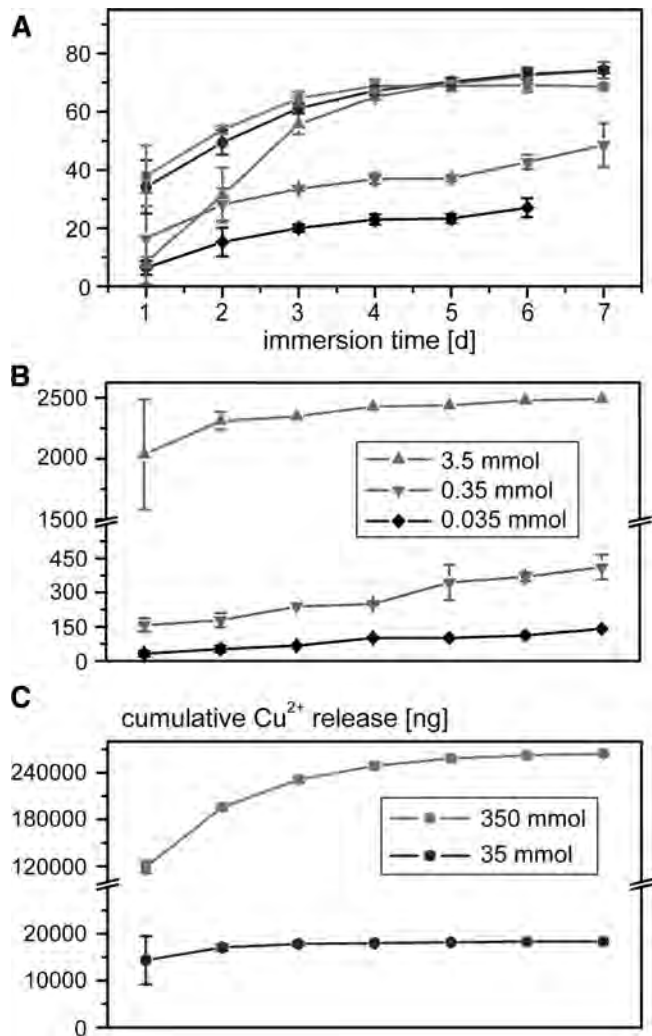


FIG. 2. Cumulative copper ion release from DCPD scaffolds loaded with different amounts of copper sulfate with immersion time in (A) PBS and (B, C) in serum.

Only the lowest concentration of 35 $\mu\text{mol/L}$ led to the release of the majority of copper ions after 6 days; in contrast, with the highest concentration of 350 mmol/L (four orders of magnitude higher), the total release was found to be only 0.03% of the total (68 ng or 42 $\mu\text{mol/L}$). However, in serum most of the copper was released within 7 days for all samples and the release correlated well with the quantities adsorbed (Fig. 2B, C).

Macroscopic and histological observation

DCPD control scaffolds. Upon retrieval, the unloaded DCPD control scaffolds ($n=6$) had little wound tissue present either within the opening of the main open pores or within the smaller branches (i.e., closed and/or open pores) (Fig. 3A). Figure 3 shows the macroscopic appearance of tissue in the end of the closed pore postretrieval and a high magnification histological section of tissue removed from the end of the closed pore. This tissue was very fragile; hence, only a small amount was retrieved intact from the pore for histological analysis. Histological sections demonstrated poor vessel development after 15 days with tissue that resembled an aged fibrin clot (reddish pink); many rounded cells were found showing morphological characteristics suggestive of inflammatory cells (Fig. 3A).

DCPD scaffolds loaded with angiogenic factors. Scaffolds loaded with copper sulfate (Fig. 3B–D) also appeared to contain inflammatory cells, but microvessels were observed at low and intermediate doses (Fig. 3B, C). The tissue from the closed pore of the scaffold with an intermediate dose also contained cells with elongated nuclei and cytoplasm, suggestive of fibroblasts (Fig. 3C). At high copper doses (Fig. 3D) no vessels were observed and fibrin appeared to be present as was observed in the control. Histology of tissue removed from the end of the closed pore of scaffolds loaded with VEGF revealed rounded cells and microvessels, and no fibrin was observed. There appeared to be more vessels apparent in scaffolds loaded with 2 μg of VEGF than with 200 ng (Fig. 3F and 3E, respectively). After a 15-day implantation period scaffolds loaded with 0.2 μg VEGF and 56 ng of copper were infiltrated with vascularized tissue (Fig. 3G) that was histologically similar to tissue retrieved from scaffolds treated with VEGF alone.

Immunohistochemistry. Wound tissues retrieved from the closed pore of the unloaded control scaffolds did not reveal any obvious microvessels as confirmed by the absence of CD31-positive cells (Fig. 4A). However, numerous microvessels were observed in samples treated with low and intermediate doses of copper sulfate (Fig. 4B, C) and with VEGF (Fig. 4D).

Tissue ingrowth and microvessel migration. Scaffolds containing angiogenic factors, especially 560 ng of copper and the copper–VEGF combination, were observed to have a greater degree of wound tissue ingrowth than the control. However, attempts to quantify this were not successful mainly because of the practical difficulty in removing and mounting these tissues intact. Indeed, wound tissue was never removed in one piece, but rather two or more fragments. An additional confounding factor was tissue

shrinkage during processing. Nevertheless, this finding was consistently observed in between five and eight replicate scaffolds per condition examined.

In the control scaffolds, migration of microvessels was mainly limited to the first 1–3 mm from the opening of the main open pores, and in some instances into the small pore branch opening (Fig. 5). In the presence of all angiogenic factors, microvessels had migrated significantly further toward the closed pore end compared with control scaffolds ($p \leq 0.05$) (Figs. 5 and 6). When loaded with 0.2 μg of VEGF, the microvessel invasion was significantly different than that of the control and the 5.6 μg copper sulfate–loaded scaffolds. The higher dose of VEGF (2 μg) significantly increased the microvessel migration compared to control and scaffolds loaded with 5.6 μg and 560 ng copper sulfate; similar results were also found with the combination of low doses of copper sulfate and VEGF.

Discussion

Using a DCPD material designed with localized adsorption of VEGF or copper ions in the interior of a 3D fabricated macroporous scaffold, it was possible to induce wound tissue infiltration and guidance of vascularization. The cumulative release of copper ions from the DCPD scaffolds after 1 week of immersion in PBS was much reduced except in the lowest doses (Fig. 2 and Table 1) compared to serum. The limited release of copper was unexpected because copper sulfate is highly water soluble and might be explained by a reaction with the brushite matrix that forms both $\text{CaSO}_4 \cdot 2\text{H}_2\text{O}$ and $\text{Cu}_3(\text{PO}_4)_2$. $\text{Cu}_3(\text{PO}_4)_2$ and has a solubility product of $10\text{--}37 \text{ mol}^5\text{L}^{-5}$, which corresponds to a copper ion concentration of $2.98 \times 10^{-6} \text{ g/L}$ in a saturated copper phosphate solution.²⁴ This concentration of 2.98 $\mu\text{g/L}$ (2.98 ppb) is approximately 30 ng in 10 mL PBS and fits well with the released amounts from the matrices (Fig. 2). This chemically bound copper is thought to be only released in higher concentrations when the brushite matrix is degraded after longer implantation *in vivo*; this was confirmed by release data collected in serum (Fig. 2B, C). Previous studies have confirmed the higher solubility of brushite cements in serum, so dissolution of the matrix is thought to be the mechanism of copper release in this case, and inhibition of insoluble apatite formation was thought to be the reason for this effect.²⁵ In addition, elevated doses (5.6 mg) of copper penetrated deep into the DCPD scaffolds and diffused beyond the region of initial application (Fig. 1A). Figure 2 shows that DCPD cement scaffolds provided sustained copper release rather than a burst release that may cause tissue toxicity, especially *in vitro* where medium volumes are low. This system therefore has interesting potential for tissue engineering applications in which seeded cells can survive in the presence of an insoluble copper ion matrix.

In this study, we found that copper sulfate deposited at levels of 56 and 560 ng per scaffold elicited an angiogenic response; this corresponded to 22 and 220 ng of copper ions, which were considerably lower than those reported in previous studies using hydrogels made of crosslinked hyaluronic acid.¹⁹ In this prior study, a range of 24 μg copper ion concentration stimulated endothelial cell growth in cultures, and 75 $\mu\text{g/g}$ of scaffold had an angiogenic potential upon implantation of hyaluran–copper composite hydrogels.

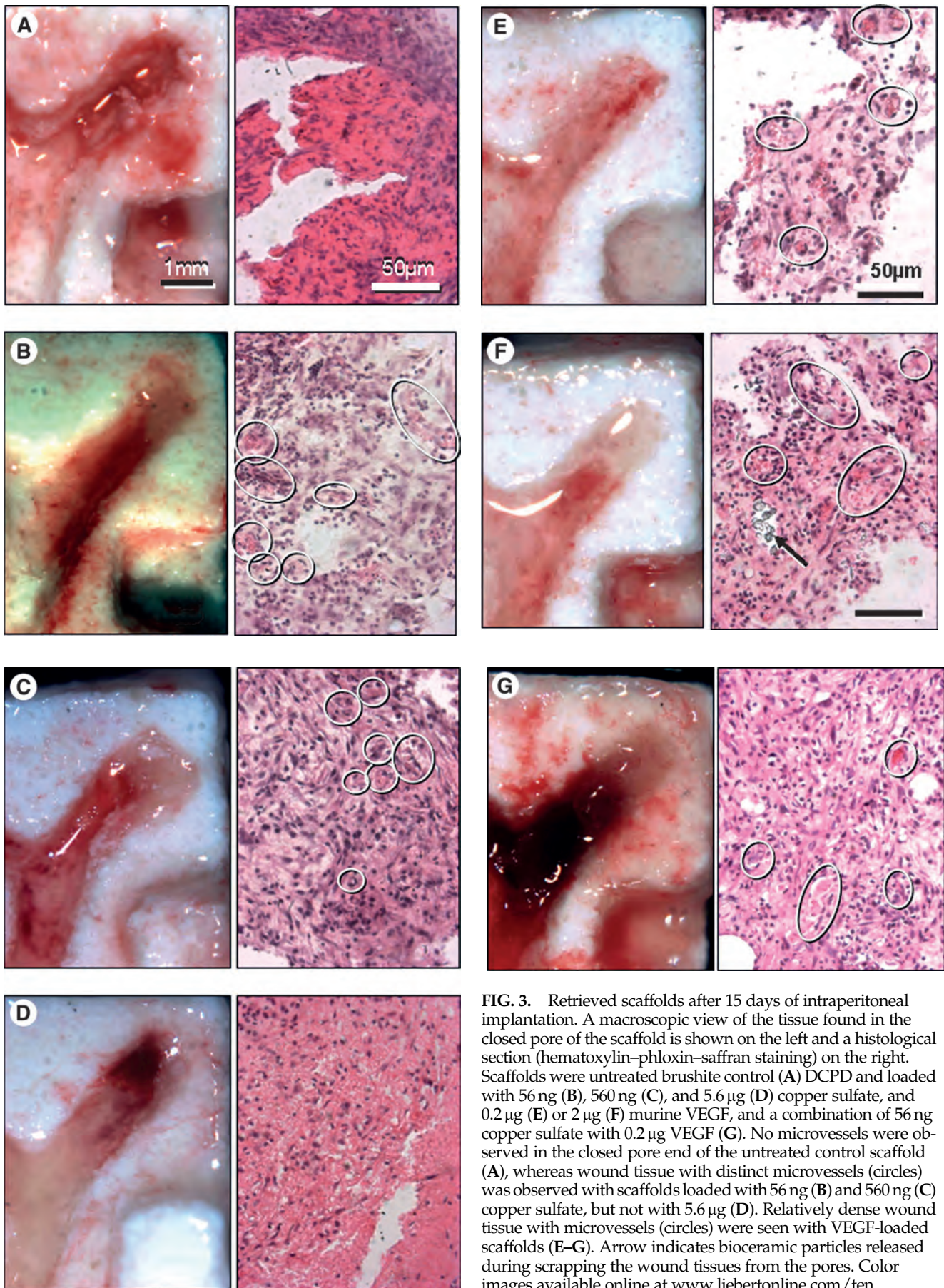


FIG. 3. Retrieved scaffolds after 15 days of intraperitoneal implantation. A macroscopic view of the tissue found in the closed pore of the scaffold is shown on the left and a histological section (hematoxylin–phloxin–safran staining) on the right. Scaffolds were untreated brushite control (A) DCPD and loaded with 56 ng (B), 560 ng (C), and 5.6 µg (D) copper sulfate, and 0.2 µg (E) or 2 µg (F) murine VEGF, and a combination of 56 ng copper sulfate with 0.2 µg VEGF (G). No microvessels were observed in the closed pore end of the untreated control scaffold (A), whereas wound tissue with distinct microvessels (circles) was observed with scaffolds loaded with 56 ng (B) and 560 ng (C) copper sulfate, but not with 5.6 µg (D). Relatively dense wound tissue with microvessels (circles) were seen with VEGF-loaded scaffolds (E–G). Arrow indicates bioceramic particles released during scrapping the wound tissues from the pores. Color images available online at www.liebertonline.com/ten.

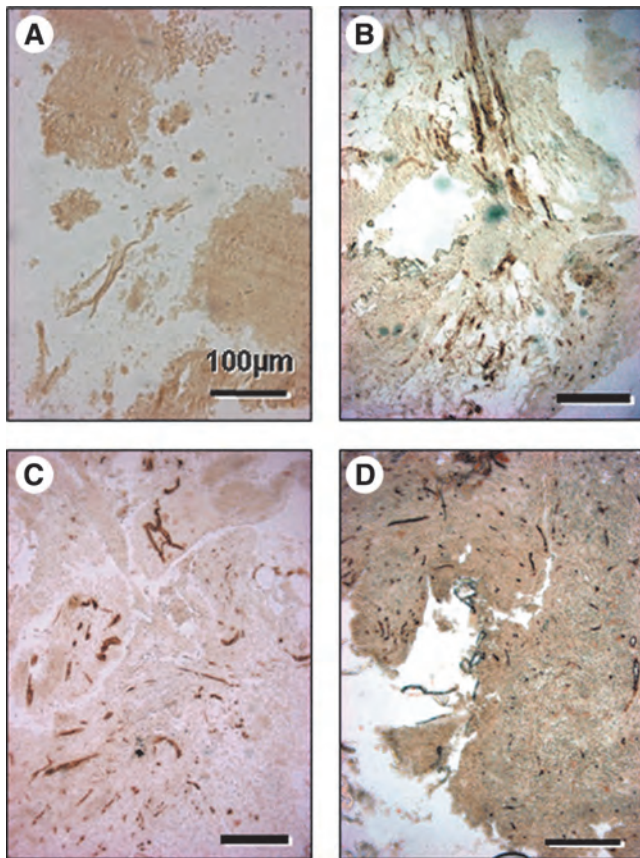


FIG. 4. Immunohistochemical staining with CD31 antibody for endothelial cells of tissue excised from the end of the closed pore of an unloaded control scaffold (A), 56 ng copper (B), 560 ng of copper (C), and 0.2 μ g VEGF and 56 ng Cu combined (D). Color images available online at www.liebertonline.com/ten.

Additionally, the angiogenic property of copper was also demonstrated in the corneal pocket assay in which 1–100 μ mol/L copper sulfate induced neovascularization *in vivo*.¹² A high dose (i.e., 500 μ mol/L) was also used to demonstrate *in vitro* that proliferation of human endothelial cells was stimulated by copper ions independently of the presence of any angiogenic growth factor.¹³ Our results suggest that low doses, in the order of ng, of copper sulfate are more than enough to be efficient in stimulating angiogenesis, possibly due to localization in the pores within the interior of DCPD scaffolds.

Among different doses of copper, very low doses of copper sulfate, such as 56 ng per scaffold, optimized angiogenesis during tissue ingrowth; whereas a 10-fold increase in the dose (i.e., 560 ng per scaffold) enhanced wound tissue ingrowth. Copper sulfate in the closed branch may have had a chemotactic capacity for wound tissue as the tissue was highly localized in this branch, and the ability of copper to induce endothelial cell migration and proliferation *in vitro* has been reported previously.^{13,26} Although there was no evidence of inflammation at these low copper doses, the possibility that the induction of blood vessel formation was not through physiological angiogenesis cannot be discounted. Sometimes inflammation can cause localized blood

vessel formation as has been observed during the degradation of polymeric α -hydroxyl acid implants and hydrogels.^{27,28} However, practically speaking, this makes little difference because the goal was to accelerate blood vessel ingrowth into the porous implants. Further study may elucidate the precise mechanism by which copper induces blood vessel formation.

Similarly, VEGF loaded at the closed branch also induced wound tissue ingrowth from outside the scaffold. However, the formation of microvessels within the pore loaded with copper sulfate did not reach the same extent as that obtained by VEGF (Fig. 6). Fibrin was routinely present in control scaffolds, with little vascular ingrowth; therefore, these observations demonstrate the bioactivity of the angiogenic compounds introduced in the closed pores. It has been previously demonstrated that copper sulfate–induced VEGF expression *in vitro* in keratinocytes and endothelial cells and *in vivo* in a skin flap model by enhancing cell viability, angiogenesis, and skin flap survival.^{14,29} Further, copper allows the release of growth factors (e.g., FGF-1, FGF-2, Interleukin (IL)- α , and probably VEGF) from producing cells by binding to proteins of the cell membrane releasing complex.³⁰ This suggests that copper acts as cofactor to amplify endothelial cell activity. Thus, another action of copper will be to trigger, for example, endothelial cells preseeded in the porosity of a scaffold in which angiogenesis can be activated.

Loading DCPD scaffolds with VEGF at a specific site (i.e., closed branch) enhanced angiogenesis and guidance of microvessels, probably by forming a gradient from the large and small open pore toward the closed branch in the Y-shaped channel. Although the presence of VEGF did enhance wound tissue ingrowth, the response appeared limited compared to the response with 560 ng copper sulfate, the latter being significantly greater than that of the control scaffold. It was only when VEGF was combined to copper sulfate, at least at low doses, that a significant effect on wound healing and angiogenesis was observed (Figs. 3G and 6). To our knowledge, the combination of VEGF and copper into a scaffold has not been previously investigated. It may be a very interesting concept because low doses can be used and each component seems complementary toward vascularized wound tissue formation. In addition, collagenase activity has been found to increase in the presence of copper and this may assist endothelial cells to migrate through extracellular matrices.³¹ Both concepts are interesting in bone repair and tissue engineering design in which cells (e.g., vascular endothelial cells) seeded into reconstituted extracellular matrix such as collagen gel can enhance tissue remodeling.

Conclusions

In comparison with previous studies using a crosslinked hyaluronic acid hydrogel to bind copper,¹⁹ our study demonstrates that it is possible, using about 1000-fold lower doses, to guide a vascularized wound tissue during its migration into a porous structure. Because high levels of copper may be toxic, this significant reduction in the amount of copper exposed to cells and biological tissues without a compromise in the proangiogenic, and healing effect is an important finding. In addition, the presence of wound tissue

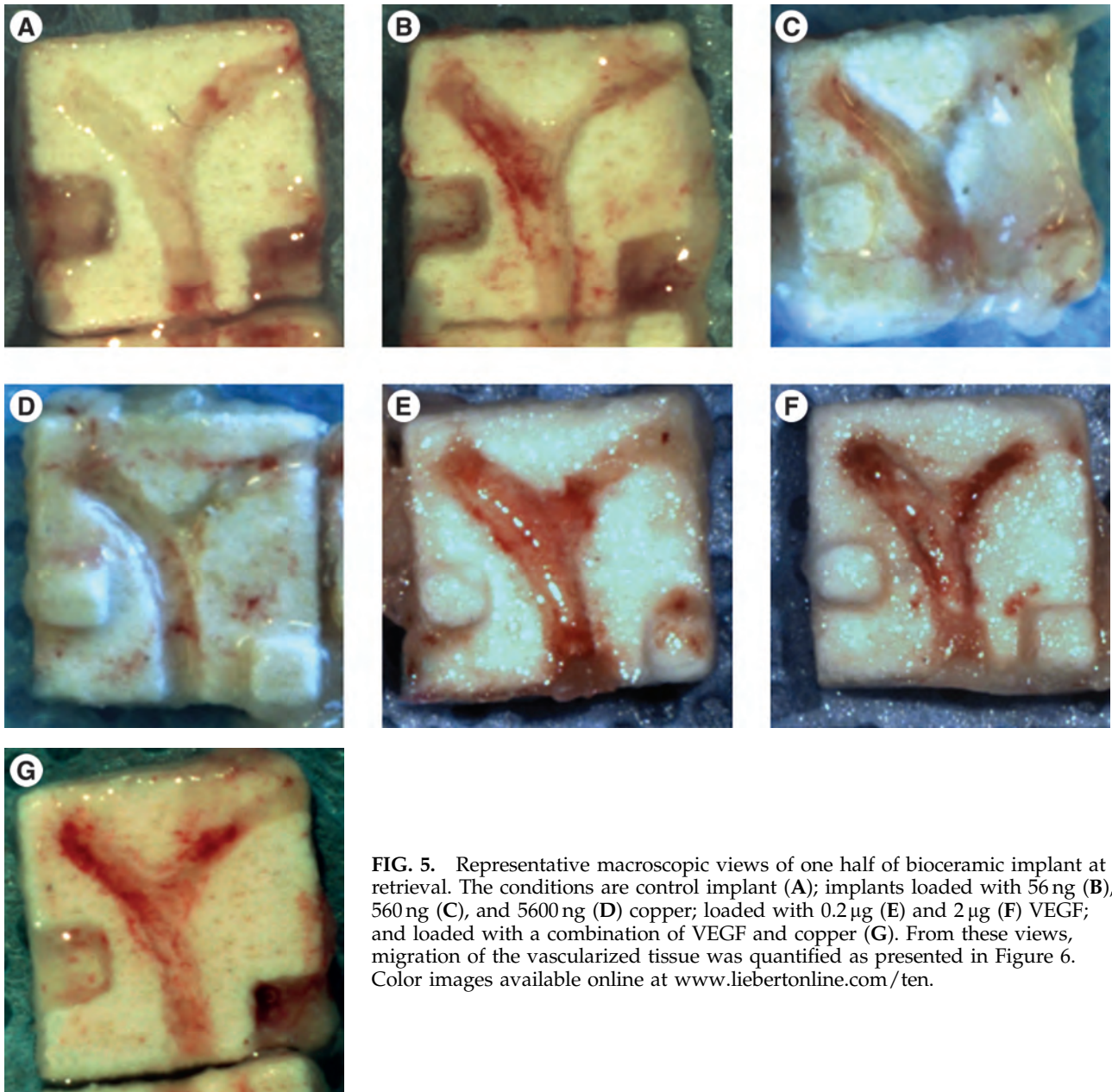


FIG. 5. Representative macroscopic views of one half of bioceramic implant at retrieval. The conditions are control implant (A); implants loaded with 56 ng (B), 560 ng (C), and 5600 ng (D) copper; loaded with 0.2 μg (E) and 2 μg (F) VEGF; and loaded with a combination of VEGF and copper (G). From these views, migration of the vascularized tissue was quantified as presented in Figure 6. Color images available online at www.liebertonline.com/ten.

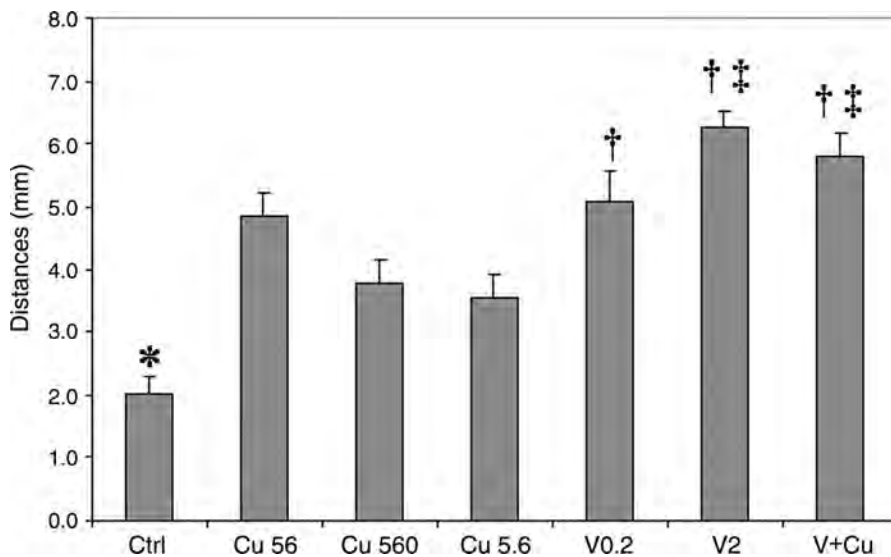


FIG. 6. Mean distance of microvessel ingrowth from the main pore opening to the closed end pores (dashed circle and asterisk in Fig. 1A) after 15 days of implantation. Control implants (Ctrl; $n = 6$), scaffolds loaded with 56 ng (Cu 56; $n = 5$), 560 ng (Cu 560; $n = 4$), and 5.6 μg (Cu 5.6; $n = 4$) copper sulfate per scaffold. Other scaffolds were preloaded with 0.2 μg (V0.2; $n = 6$) and 2 μg (V2; $n = 3$) and with a combination of 0.2 μg VEGF and 56 ng copper sulfate (V+Cu; $n = 5$). Error bars indicate standard errors of the mean. *Control condition significantly different ($p \leq 0.05$) compared with the other conditions; †compared with Cu 5.6; and ‡compared with Cu 560.

in the whole Y-shaped pore of the copper-loaded DCPD scaffolds suggests a chemotactic effect of copper sulfate. Thus, copper-loaded DCPD scaffolds not only provided directional vascularization but also enhanced wound healing. Further, the strategies demonstrated here are useful for the design of a wide range of tissue-engineered systems in which angiogenesis and vasculogenesis as well as osteogenesis can be preestablished before implantation and therefore enhancing bone regeneration and repair. The use of stable and low-cost inorganic copper ions to induce a regenerative response within scaffolds offers a complementary approach to the use of recombinant or concentrated protein or peptide growth factors.

Acknowledgments

This work was supported in part by a Quebec-Bavarian support grant from the “Développement économique, innovation et exportation” of Québec, Canada, by the Canadian Institute of Health Research and a Canada Research Chair (J.B.) and by the Bavarian Government (Bavaria-Quebec grant No. 9.305 “Knochenimplantate”).

Disclosure Statement

No competing financial interests exist.

References

- Nomi, M., Atala, A., Coppi, P.D., and Soker, S. Principals of neovascularisation for tissue engineering. *Mol Asp Med* **23**, 463, 2002.
- Muschler, G.F., Nakamoto, C., and Griffith, L.G. Engineering principles of clinical cell-based tissue engineering. *J Bone Joint Surg Am* **86**, 1541, 2004.
- Kannan, R.Y., Salacinski, H.J., Sales, K., Butler, P., and Seifalian, A.M. The roles of tissue engineering and vascularisation in the development of micro-vascular networks: a review. *Biomaterials* **26**, 1857, 2005.
- Shepherd, B.R., Enis, D.R., Wang, F., Suarez, Y., Pober, J.S., and Schechner, J.S. Vascularization and engraftment of a human skin substitute using circulating progenitor cell-derived endothelial cells. *FASEB J* **20**, 1739, 2006.
- Ito, H., Koefoed, M., Tiyapatanaputi, P., Gromov, K., Goater, J.J., Carmouche, J., Zhang, X., Rubery, P.T., Rabinowitz, J., Samulski, R.J., Nakamura, T., Soballe, K., O’Keefe, R.J., Boyce, B.F., and Schwarz, E.M. Remodeling of cortical bone allografts mediated by adherent rAAV-RANKL and VEGF gene therapy. *Nat Med* **11**, 291, 2005.
- Eriksen, E.F., Eghbali-Fatourehchi, G.Z., and Khosla, S. Remodeling and vascular spaces in bone. *J Bone Miner Res* **22**, 1, 2007.
- Huang, K.K., Shen, C., Chiang, C.Y., Hsieh, Y.D., and Fu, E. Effects of bone morphogenetic protein6 on periodontal wound healing in a fenestration defect of rats. *J Periodontal Res* **40**, 1, 2005.
- Poole, T.J., Finkelstein, E.B., and Cox, C.M. The role of FGF and VEGF in angioblast induction and migration during vascular development. *Dev Dyn* **220**, 1, 2001.
- Kaigler, D., Wang, Z., Horger, K., Mooney, D.J., and Krebsbach, P.H. VEGF scaffolds enhance angiogenesis and bone regeneration in irradiated osseous defects. *J Bone Miner Res* **21**, 735, 2006.
- Smith, M.K., Peters, M.C., Richardson, T.P., Garbern, J.C., and Mooney, D.J. Locally enhanced angiogenesis promotes transplanted cell survival. *Tissue Eng* **10**, 63, 2004.
- Silva, E.A., and Mooney, D.J. Spatiotemporal control of vascular endothelial growth factor delivery from injectable hydrogels enhances angiogenesis. *J Thromb Haemost* **5**, 590, 2007.
- Parke, A., Bhattacharjee, P., Palmer, R.M.J., and Lazarus, N.R. Characterization and quantification of copper sulfate-induced vascularization of the rabbit cornea. *Am J Pathol* **130**, 173, 1988.
- Hu, G. Copper stimulates proliferation of human endothelial cells under culture. *J Cell Biochem* **69**, 326, 1998.
- Sen, C.K., Khanna, S., Venojarvi, M., Trikha, P., Ellison, E.C., Hunt, T.K., and Roy, S. Copper-induced vascular endothelial growth factor expression and wound healing. *Am J Physiol Heart Circ Physiol* **282**, H1821, 2002.
- Goodman, V.L., Brewer, G.J., and Merajver, S.D. Control of copper status for cancer therapy. *Curr Cancer Drug Targets* **5**, 543, 2005.
- Halliwell, B., and Gutteridge, J.M.C. Role of free-radicals and catalytic metal-ions in human-disease—an overview. *Methods Enzymol* **186**, 1, 1990.
- Arredondo, M., and Nunez, M.T. Iron and copper metabolism. *Mol Aspects Med* **26**, 313, 2005.
- Barbucci, R., and Magnani, A. Metal-ion complexes in the angiogenetic effect. *Macromol Symp* **156**, 239, 2000.
- Giavaresi, G., Torricelli, P., Fornasari, P.M., Giardino, R., Barbucci, R., and Leone, G. Blood vessel formation after soft-tissue implantation of hyaluronan-based hydrogel supplemented with copper ions. *Biomaterials* **26**, 3001, 2005.
- Murphy, W.L., Simmons, C.A., Kaigler, D., and Mooney, D.J. Bone regeneration via a mineral substrate and induced angiogenesis. *J Dent Res* **83**, 204, 2004.
- Kaigler, D., Wang, Z., Horger, K., Mooney, D.J., and Krebsbach, P.H. VEGF scaffolds enhance angiogenesis and bone regeneration in irradiated osseous defects. *J Bone Miner Res* **21**, 735, 2006.
- Leach, J.K., Kaigler, D., Wang, Z., Krebsbach, P.H., and Mooney, D.J. Coating of VEGF-releasing scaffolds with bioactive glass for angiogenesis and bone regeneration. *Biomaterials* **27**, 3249, 2006.
- Gbureck, U., Hölzel, T., Doillon, C.J., Müller, F.A., and Barralet, J.E. Direct printing of bioceramic implants with spatially localized angiogenic factors. *Adv Mater* **19**, 795, 2007.
- Drogowska, M., Brossard, L., and Menard, H. Comparative study of copper behaviour in bicarbonate and phosphate aqueous solutions and effect of chloride ions. *J Appl Electrochem* **24**, 344, 1994.
- Grover, L.M., Knowles, J.C., Fleming, G.J.P., and Barralet, J.E. *In vitro* ageing of brushite calcium phosphate cement. *Biomaterials* **24**, 4133, 2003.
- McAuslan, B.R., Reilly, W.G., Hannan, G.N., and Gole, G.A. Angiogenic factors and their assay—activity of formyl methionyl leucyl phenylalanine, adenosine-diphosphate, heparin, copper, and bovine endothelium stimulating factor. *Microvasc Res* **26**, 323, 1983.
- Chevrier, A., Hoemann, C.D., Sun, J., and Buschmann, M.D. Chitosan-glycerol phosphate/blood implants increase cell recruitment, transient vascularization and subchondral bone remodeling in drilled cartilage defects. *Osteoarthritis Cartilage* **15**, 316, 2007.

28. Sung, H., Meredith, C., Johnson, C., and Galis, Z.S. The effect of scaffold degradation rate on three-dimensional cell growth and angiogenesis. *Biomaterials* **25**, 5735, 2004.
29. Frangoulis, M., Georgiou, P., Chrisostomidis, C., Perrea, D., Dontas, I., Kavantzas, N., Kostakis, A., and Papadopoulos, O. Rat epigastric flap survival and VEGF expression after local copper application. *Plast Reconstr Surg* **119**, 837, 2007.
30. Sivaraja, V., Kumar, T.K., Rajalingam, D., Graziani, I., Prudovsky, I., and Yu, C. Copper binding affinity of S100A13, a key component of the FGF-1 non classical copper-dependent release complex. *Biophys J* **91**, 1832, 2006.
31. Lin, M.T., and Chen, Y.L. Effect of copper-ion on collagenase release—its implication in corneal vascularization. *Invest Ophthalmol Vis Sci* **33**, 558, 1992.

Address correspondence to:
 Charles J. Doillon, Ph.D., M.D.
Oncology and Molecular Endocrinology Research Centre
 (T3-63)
 CHUL Research Centre
 CHUQ, 2705 Blvd. Laurier
 Quebec City
 Quebec G1V 4G2
 Canada

E-mail: charles.doillon@crchul.ulaval.ca

Received: November 6, 2007

Accepted: October 15, 2008

Online Publication Date: January 26, 2009

